Structural Engineering and Mechanics, *Vol. 73, No. 6 (2020) 641-649*
DOI: https://doi.org/10.12989/sem.2020.73.6.641

Study on midtower longitudinal stiffness of three-tower four-span suspension bridges with steel truss girders

Jin Cheng*[1,2], Hang Xu[2a] and Mingsai Xu[2a]

[1]*State Key Laboratory for Disaster Reduction in Civil Engineering, Tongji University, Shanghai, China*
[2]*Department of Bridge Engineering, Tongji University, Shanghai, China*

(*Received January 9, 2019, Revised October 17, 2019, Accepted November 12, 2019*)

Abstract. The determination of midtower longitudinal stiffness has become an essential component in the preliminary design of multi-tower suspension bridges. For a specific multi-tower suspension bridge, the midtower longitudinal stiffness must be controlled within a certain range to meet the requirements of sliding resistance coefficient and deflection-to-span ratio. This study presents a numerical method to divide different types of midtower and determine rational range of longitudinal stiffness for rigid midtower. In this method, influence curves of midtower longitudinal stiffness on sliding resistance coefficient and maximum vertical deflection-to-span ratio are first obtained from the finite element analysis. Then, different types of midtower are divided based on the regression analysis of influence curves. Finally, rational range for longitudinal stiffness of rigid midtower is derived. The Oujiang River North Estuary Bridge which is a three-tower four-span suspension bridge with two main spans of 800m under construction in China is selected as the subject of this study. This will be the first three-tower four-span suspension bridge with steel truss girders and concrete midtower in the world. The proposed method provides an effective and feasible tool for engineers to design midtower of multi-tower suspension bridges.

Keywords: three-tower suspension bridges; midtower; longitudinal stiffness; sliding resistance; deflection-to-span ratio

1. Introduction

With ever-increasing traffic demand and recent development in construction techniques, a number of sea-crossing engineering have been placed on the agenda. Due to their long span capability, structural efficiency and cost savings, multi-tower suspension bridges have become the most economic solution when crossing deep straits or rivers that are more than 2km wide (Choi *et al*. 2013, Zhang *et al*. 2013a, 2013b). Before 2000, only two multi-tower suspension bridges with spans over 100 meters was built. One is the Konaruto Bridge with two 160-m main spans built in Japan in 1961, and the other is the Save River Bridge with three main spans of 210m built in Mozambique in 1965 (Ge and Xiang 2011). Recently, a number of long-span multi-tower suspension bridges were successfully constructed, including Taizhou Yangtze River Bridge (390+1080+1080+390 m), Maanshan Yangtze River Bridge (360+1080+1080+360 m), Yingwuzhou Yangtze River Bridge (200+850+850+200 m) in China and New Millennium Grand Bridge (225+650+650+225 m) in Korea (Jung *et al*. 2010), and some others are under construction such as Oujiang River North Estuary Bridge (230+800+800+348 m) in China.

Compared with the conventional suspension bridge, the multi-tower suspension bridge has significant differences in structural characteristics and mechanical behavior (Fukuda 1976, Collings 2016, Forsberg 2001, Thai and Choi 2013, Ma *et al*. 2016, Choi *et al*. 2013, Ruan *et al*. 2016, Daniel *et al*. 2010, Zhang *et al*. 2012). The horizontal stiffness of the main cable at the side span is always much larger than that at the main span, in other words, the constraint from the main cable in the midtower of multi-tower suspension bridge is less effective than that in the towers in a two-tower suspension bridge. Consequently, the multi-tower suspension bridge has lower overall stiffness and usually endure a much larger live load deflection than conventional suspension bridge with the same structural parameters (Wang and Chai 2018). The use of rigid midtower in multi-tower suspension bridges is an effective method to increase the overall structural stiffness (Yoshida 2004, Zhang *et al*. 2018). However, increasing the midtower stiffness may lead to sliding of the main cable at the tower saddles under unbalanced cable tension on both sides of the tower, and thus the antiskid stability of the main cable would be reduced (Wang *et al*. 2017, Ruan *et al*. 2016, Kim *et al*. 2012, Takena *et al*. 1992). Fortunately, some solutions have been proposed to improve sliding resistance of the main cable in the midtower saddle. Hasegawa *et al*. (1995) proposed the use of a horizontal friction plate in the saddle to enhance the sliding resistance while Zhang *et al*. (2017) and Cheng *et al*. (2018) proposed to use vertical friction plates, and these methods have been proved effective in improving sliding resistance of the main cable. Therefore, rigid concrete midtower is gradually adopted in multi-tower suspension bridges, such as the Oujiang River North Estuary Bridge.

In research for the midtower of multi-tower suspension

*Corresponding author, Professor
E-mail: chengjin@tsinghua.org.cn
[a] M.S. Student

http://www.techno-press.com/journals/sem&subpage=7
ISSN: 1225-4568 (Print), 1598-6217 (Online)

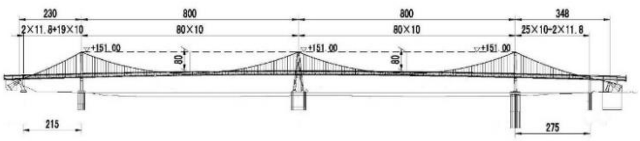

Fig. 1 Elevation view of the Oujiang River North Estuary Bridge (unit: m)

Table 1 Structural parameters of Oujiang River North Estuary Bridge

Item	Parameter	Value
Cable	Cross sectional area	2.459 m^2
	Tensile strength	1860 MPa
Hanger	Diameter	0.083 m
	Tensile strength	1770 MPa
Girder	Moment of inertia	87.6 m^4

bridges, Choi *et al*. (2014) proposed an equivalent model for the preliminary analysis and design of suspension bridge towers. Ma *et al*. (2016) established the kinematic multispring model in which tower springs and cable springs constitute a series-parallel system to investigate longitudinal stiffness of multi-tower suspension bridges. Wang and Chai (2018) presented a set of formulas to determine the midtower stiffness in an in-plane double-cable three-tower suspension bridge. Cao (2018) investigated the structural characteristics of midtowers in three-tower suspension bridges and proposed an approach to determine the feasible midtower stiffness using a simplified bridge model. As revealed from the above literature review, the majority of previous research on midtowers in multi-tower suspension bridges focused on the analytical theory of this new structural system while few studies were concerned about the classification of different types of midtower, and more importantly, the determination of rational range for midtower stiffness in preliminary designs.

This paper developed a numerical method to divide different types of midtower and determine rational range of longitudinal stiffness for rigid midtower based on the Oujiang River North Estuary Bridge. In this method, influence curves of midtower longitudinal stiffness on sliding resistance coefficient and maximum vertical deflection-to-span ratio are first obtained from the finite element analysis. Then, different types of midtower are divided based on the regression analysis of influence curves. Finally, rational range for longitudinal stiffness of rigid midtower is derived.

The remainder of this paper is structured as follows. The description of example three-tower suspension bridge and the modeling process are first presented in Section 2; Section 3 reviews the concept of sliding resistance coefficient and deflection-to-span ration which are both susceptible to the variation of midtower longitudinal stiffness; Section 4 illustrates the influence of midtower longitudinal stiffness on sliding resistance coefficient and maximum vertical deflection-to-span ratio and performs the regression analysis of influence curves. Section 5 proposes an analytical approach to divide different intervals of midtower longitudinal stiffness based on the results of regression analysis; In Section 6, a rational range for longitudinal stiffness of rigid midtower defined in Section 5 is investigated; finally, some conclusions are drawn in Section 7.

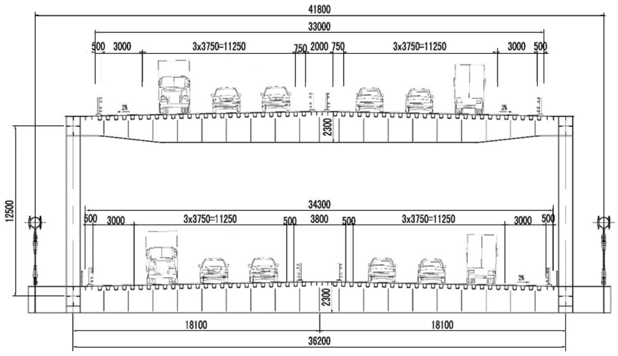

Fig. 2 Bridge deck of the Oujiang River North Estuary Bridge (unit: mm)

2. Example suspension bridge

2.1 Bridge description

Oujiang River North Estuary Bridge is a three-tower four-span suspension bridge with steel truss girders under construction in Wenzhou, China. This will be the first three-tower suspension bridge with steel truss girders and concrete midtower in the world. Fig. 1 shows the elevation view of this bridge and Table 1 lists the structural parameters of the bridge. The anchorage-to-anchorage bridge span arrangements are (230+800+800+348) m; the cable sag is one-tenth of the main-span length; the distance between the two cables is 41.8m; the cross-sectional area of the cable is 2.459 m^2; the hanger has a diameter of 0.083 m; the longitudinal spacing between the two hangers is 10m in standard segments and 11.8 m in the segments of the end area of side span.

The continuous stiffening girder system is used in this bridge and the stiffening girder is a double-deck steel truss girder with 12.5 m depth, as shown in Fig. 2; the geometric arrangements for the main truss is the Warren type; width between center lines of the two main trusses is 36.2 m; upper and lower chords are designed as a closed box while H-section is used in verticals and diagonals. The bridge upper and lower decks are made of orthotropic steel plates with 16-mm depth, reinforced by longitudinal trapezoidal shaped ribs and diaphragms with an inverted T-section; diaphragm spacing arrangements are 3.3+3.4+3.3 m within one panel length; the trapezoidal shaped rib is 280 mm high and spaced 600 mm; the wall thickness of trapezoidal shaped rib is 8 mm; the width of trapezoidal shaped rib at the top and bottom are 300 mm and 180 mm, respectively; the upper deck is used for six-lane expressway route and the lower deck is used as the six-lane highway route.

The midtower is a reinforced concrete pylon with a portal frame in the lateral view and A-shaped type in the longitudinal direction while the two side towers are portal

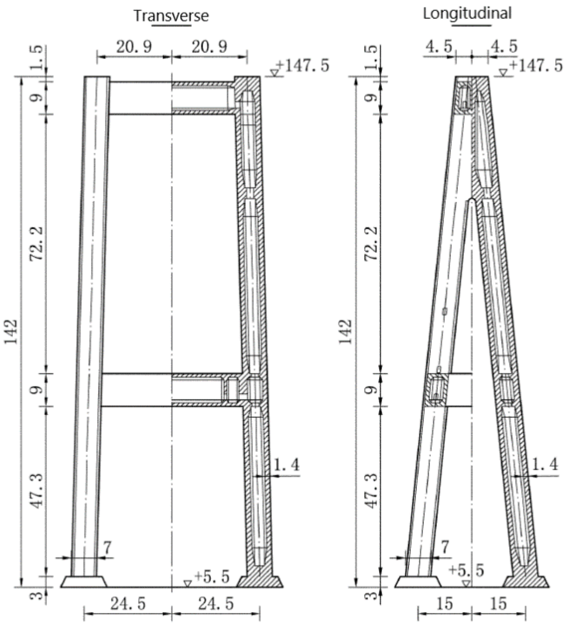

Fig. 3 Midtower of the Oujiang River North Estuary Bridge (unit: m)

reinforced concrete structures; vertical bearings are placed on lower cross beams of towers; lateral supports are installed at the joints of the tower and the main girder to resist wind loads.

As shown in Fig. 3, total height of the midtower is H=142 m; $B_1 = 7$ m and $B_2 = 7$ m are the width of each leg in longitudinal direction and transverse direction respectively; $D = 30$ m is the distance between centerlines of the two tower legs at the bottom in longitudinal direction; $L_1 = 41.8$ m is the distance between centerlines of the two tower legs at the top and $L_2 = 49$ m is the distance between centerlines of the two tower legs at the bottom in transverse direction. The designed midtower longitudinal stiffness of Oujiang River North Estuary Bridge is 4.382×10^5 kN/m.

2.2 Finite element modelling

According to the bridge design, a three-dimensional spatial truss finite element model (FEM) was firstly constructed for the Oujiang River North Estuary Bridge using MIDAS Civil software, as shown in Fig. 4. In this FEM, the three towers and components of steel truss girders including upper and lower chords, verticals and diagonals were accurately modeled by spatial beam elements while the bridge upper and lower decks were modeled by spatial shell elements. The cables and hangers were simulated by truss elements using Ernst's equivalent elastic modulus accounting for geometric nonlinearity. The truss elements were assigned tension-only.

The anchor points of the hangers at the stiffening girder were connected to the central beam by rigid body connections. The main cables were also fixed on top of the towers. As seen in the bridge design, the deck and towers were coupled in 2 degrees of freedom, including the vertical displacement and the transverse displacement. The bottom

(a) full FEM

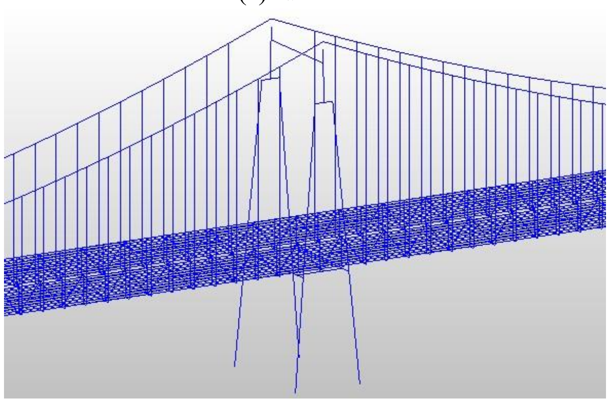

(b) middle part of the model

Fig. 4 The spatial truss FEM

(a) full FEM

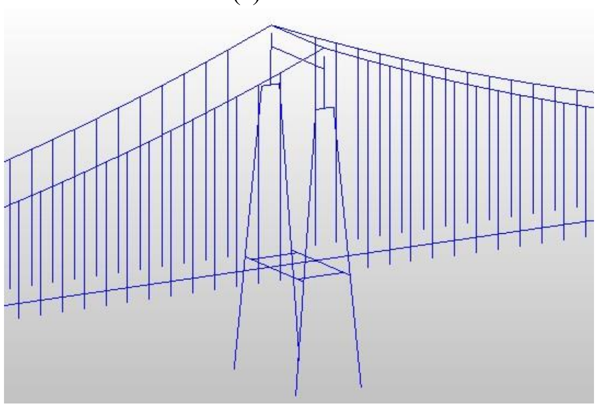

(b) middle part of the model

Fig. 5 The single-beam FEM

of both back cables and towers were fixed at the base, ignoring the soil-pile-structure interaction.

The spatial truss FEM consisted of: 22398 beam elements, 824 truss elements, 13816 shell elements, and a total of 18233 nodes. It's just very time consuming to carry out the in-depth calculations by using this model. Therefore, a single-beam FEM was then established to replace the spatial truss FEM, as shown in Fig. 5. In this model, the steel truss girder was represented by a single beam passing through the centroids of the girder sections and the cross-section properties of the stiffening girder were assigned to the beam as equivalent properties. The single-beam FEM consisted of: 388 beam elements, 808 truss elements, and a total of 1196 nodes. A geometrically nonlinear analysis considering large deflection was performed using the Newton-Raphson method with the convergence criteria of a displacement norm of 0.001 m.

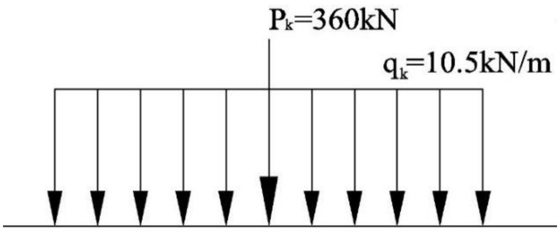

Fig. 6 The Grade-I traffic load

2.3 Model verification

To verify the validity of single-beam FEM, representative deformations under five load cases were compared between the two FEMs. Case 1 is dead load taken as 475.9 kN/m, including the first and second phases of the bridge deck. Case 2 considered is the Grade I highway traffic load in two directions proposed in the Chinese code for the design of bridges (CCCC Highway Consultants Co., Ltd.) (JTG-D60-2015 2015); the traffic load consists of a distribution load and a concentrated load, as shown in Fig. 6. Case 3 is full-length live load acting on one of the main spans. Case 4 is static wind load and Case 5 is thermal load that the temperature of the whole structures increase by 30°C. Then, vertical displacement at the middle of midspan under Case 1, maximum vertical displacement of the main girder under Case 2 and Case 3, lateral displacement at the middle of midspan under Case 4 and longitudinal displacement at the end of the main girder under Case 5 were obtained from the finite element analysis respectively.

As shown in Table 2, vertical displacement at the middle of midspan under dead load is on the scale of millimeter, therefore, the difference between results of two FEMs can be ignored. Moreover, the analysis results of displacement under Case 2-4 with single-beam FEM agree well with the results obtained with spatial truss FEM, of which the maximum difference is less than 3%. In addition, by comparing the current analysis results to those in the design documents, the deformation of the bridge are quite close to the original design results of the Oujiang River North Estuary Bridge. The single-beam FEM established is thus deemed reasonable. Considering the characteristic of the spatial truss FEM with low computational efficiency, the single-beam FEM is used to conduct the following analysis in this study.

3. Influence factors of the determination of midtower longitudinal stiffness

Sliding resistance coefficient and maximum vertical deflection-to-span ratio are both factors of utmost concern in the determination of midtower longitudinal stiffness. The Chinese code for the design of suspension bridges (CCCC Highway Consultants Co., Ltd.) (JTG/T-D65-05-2015 2015) has mandated the longitudinal stiffness of the midtower in multi-tower suspension bridge to satisfy both the requirements of the bridge deck's maximum deflection-to-span ratio and the minimum sliding resistance coefficient of the saddle under live loads. In this part, a brief review of concepts of those two influence factors is presented.

Table 2 Comparison of deformations under five load cases between the two FEMs

Load case	Deformations(m)	The spatial truss FEM	The single-beam FEM	Relative error
Case 1	vertical displacement at mid-span of main span	5.54E-03	7.58E-03	—
Case 2	maximum vertical displacement of the main girder (upward)	0.367	0.359	2.30%
	maximum vertical displacement of the main girder (downward)	1.279	1.278	0.06%
Case 3	maximum vertical displacement of the main girder	1.184	1.173	0.93%
	longitudinal displacement at the top of midtower	0.145	0.144	0.69%
Case 4	lateral displacement at mid-span of main span	0.699	0.709	1.53%
Case 5	longitudinal displacement at the end of the main girder	0.394	0.390	0.97%

*Case 1: dead load including the first and second phases of the bridge deck; Case 2: the highway load in two directions; Case 3: full-length live load acting on one of the main spans; Case 4: static wind load and Case 5: thermal load that the temperature of the whole structures increase by 30°C

3.1 Sliding resistance coefficient

The sliding resistance of the main cable in the midtower saddle is a key factor for designing multi-tower suspension bridges (Wang 2017, Forsberg 2001, Hasegawa *et al*. 1995, Takena *et al*. 1992). For a multi-tower suspension bridge, when both sides of a midtower are loaded with an unbalanced load, cable tension force on both sides of the midtower change accordingly, and the main cable slides along the saddle surface when the difference between cable tension force on the two sides of the saddle exceeds the frictional resistance between the cable and the saddle.

The sliding resistance coefficient K is used to assess the slides behavior of the cable against the saddle

$$K=\frac{\mu\theta}{\ln\left(\frac{T_1}{T_2}\right)} \tag{1}$$

where, μ is the maximum static friction coefficient; θ is the cornerite of the main cable on the saddle; T_1 is tensile force of the main cable at the tight side; T_2 is tensile force of the main cable at the loose side.

According to Eq. (1), the sliding resistance coefficient K is largely determined by static friction coefficient μ. Therefore, it is necessary for there to be enough friction force between the tower saddles and main cable to avoid sliding. The existing recommendations on suspension bridges proposes the use of a static friction coefficient of 0.15 and a sliding resistance coefficient of 2.0 for the antiskid safety of the main cable (CCCC Highway

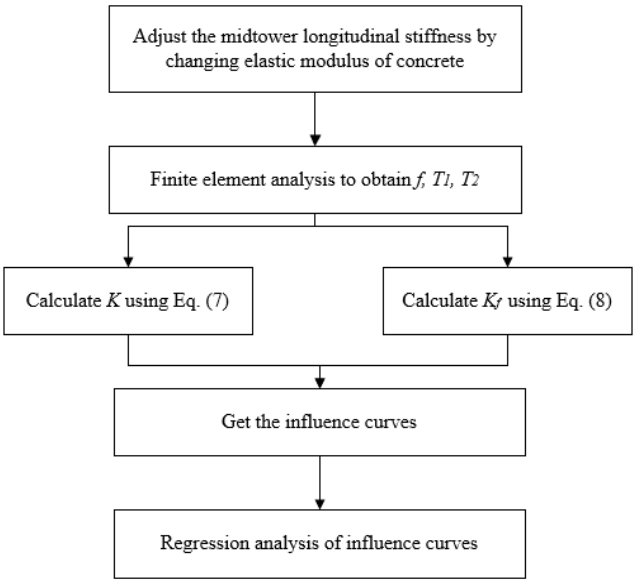

Fig. 7 Analysis procedure of the relationship between midtower longitudinal stiffness and K, K_f

Consultants Co., Ltd.) (JTG/T-D65-05-2015 2015). It is also stated in the code that a friction test is suggested if possible to optimize the values of static friction coefficient and sliding resistance coefficient.

3.2 Deflection-to-span ratio

If the midtower stiffness is insufficient, considerable deflections can be created in the main girder under service conditions, making it unsmooth and uncomfortable for driving (Ruan *et al*. 2016). The Chinese code for the design of suspension bridges (CCCC Highway Consultants Co., Ltd.) (JTG/T-D65-05-2015 2015) has imposed a limit on the maximum vertical deflection-to-span ratio, K_f, defined by Eq. (2), to be below 1/250.

$$K_f = \frac{f}{L} \tag{2}$$

where f is maximum vertical displacement of the bridge girder and L is length of the corresponding span.

4. Relationship between midtower longitudinal stiffness and *K/K_f*

As mentioned previously, midtower longitudinal stiffness must be controlled within a certain range to meet the requirements of sliding resistance coefficient K and maximum vertical deflection-to-span ratio K_f for a specific multi-tower suspension bridge. To study the effects of midtower longitudinal stiffness on K and K_f, influence curves of the change of midtower longitudinal stiffness on those two factors are first obtained from the finite element analysis in this section. The antiskid stability of the main cable will be in the worst circumstance as well as the structural deformation will be maximal when the load is applied only on one main span.

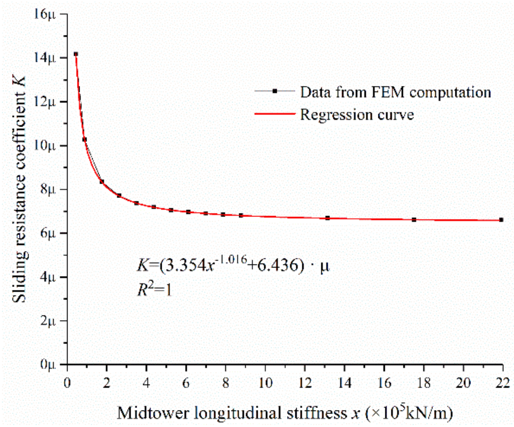

Fig. 8(a) Effect of midtower longitudinal stiffness on sliding resistance coefficient K

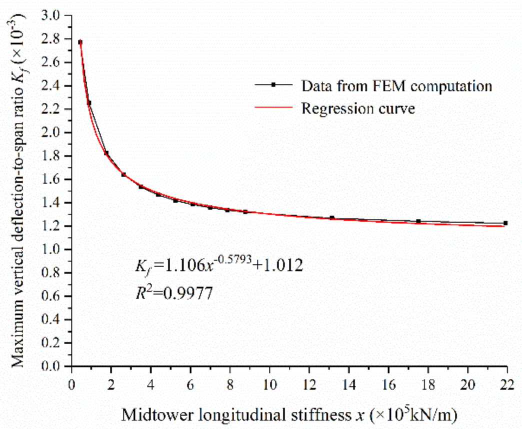

Fig. 8(b) Effect of midtower longitudinal stiffness on maximum vertical deflection-to-span ratio K_f

Therefore, the load case of full-length live load acting on one of the main spans is considered in the finite element analysis. And then regression analysis of influence curves is performed to acquire functional relationship between midtower longitudinal stiffness and K, K_f. The analysis procedure is depicted in Fig. 7.

4.1 Influence of midtower longitudinal stiffness on K and K_f

To merely investigate the influence of midtower longitudinal stiffness on sliding resistance coefficient K and maximum deflection-to-span ratio K_f, the midtower longitudinal stiffness multiple ranges from 0.1 to 5 in the FEM. The other parameters remain constant. Fig. 8(a) and Fig. 8(b) show the influence of the variation in midtower longitudinal stiffness on K and K_f, respectively.

As can be seen from Fig. 8 that increasing the midtower longitudinal stiffness will decrease the maximum vertical deflection-to-span ratio of the main girder and the sliding resistance coefficient of the main cable. The two factors significantly change when the midtower longitudinal stiffness varies from 0 to 4×10^5 kN/m and the variation rate changes very slightly with a further increase in stiffness, which indicates that the midtower longitudinal stiffness has a

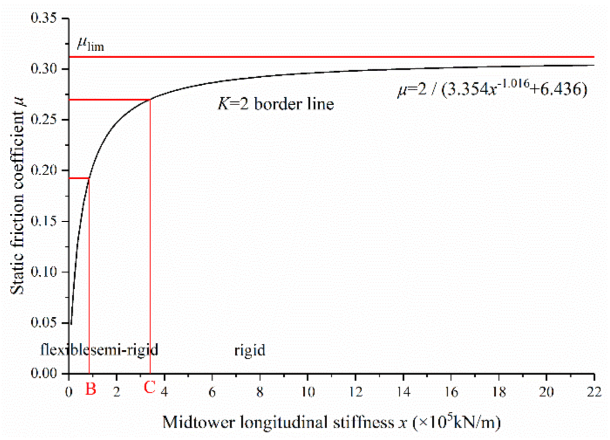

Fig. 9(a) Effect of midtower longitudinal stiffness on static friction coefficient μ required

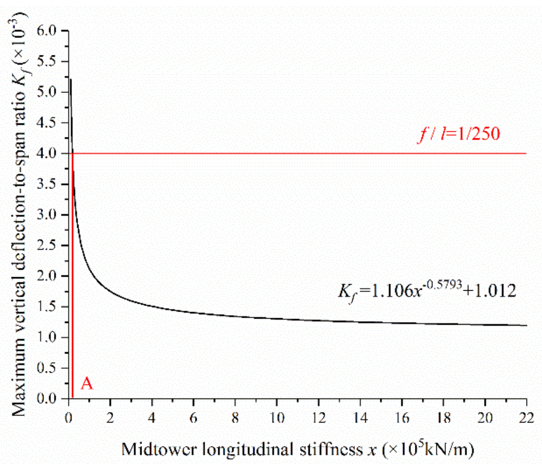

Fig. 9(b) Effect of midtower longitudinal stiffness on maximum vertical deflection-to-span ratio K_f with the limit of $K_f \leq 1/250$

greater influence on K and K_f of a bridge with a flexible midtower than a bridge with a rigid midtower.

4.2 Regression analysis of influence curves

To express explicitly the relationship between midtower longitudinal stiffness and K, K_f, regression analysis of influence curves is further conducted to get the regression curves and equations based on the Levenberg-Marquardt algorithm. The regression equations of K and K_f along with midtower longitudinal stiffness change are $K = (3.354x^{-1.016} + 6.436)\mu$, $K_f = 1.106x^{-0.5793} + 1.012$ respectively, as shown in Fig. 8. The coefficients of determination are 0.9977 and 1 respectively which indicates that the regression curves represent the data very well. In the following section, the classification of different types of midtower will be carried out based on the regression equations.

5. Different types of midtower

As shown in Fig. 8(a), the relationship among sliding resistance coefficient K, static friction coefficient μ and midtower longitudinal stiffness x can be expressed as

$$K=\left(3.354x^{-1.016}+6.436\right)\mu \tag{3}$$

When $K = 2$, functional relationship between μ and x can be derived as

$$\mu=2/\left(3.354x^{-1.016}+6.436\right) \tag{4}$$

The curve corresponding to Eq. (4) is shown in Fig. 9(a). For the region above the curve, $K > 2$, and for the region located below the curve, $K < 2$. When $x \to +\infty$, the midtower can be regarded as absolute rigid. According to Eq. (3), the minimum static friction coefficient μ_{lim} that meets the requirement of $K \geq 2$ can be obtained as shown in Fig. 9(a)

$$\mu_{\text{lim}} = \lim_{x\to+\infty,\ K=2} \frac{K}{(3.354x^{-1.016}+6.436)} = 0.312 \tag{5}$$

In other words, when $\mu = 0.312$, antiskid safety of the main cable could always be guaranteed regardless of the value of midtower longitudinal stiffness. From Fig. 9(a) it can also be seen that, when $\mu < 0.19$, the variation rate of μ that meets the requirement of $K \geq 2$ changes obviously along with midtower longitudinal stiffness change; while $\mu > 0.27$, the variation rate of μ that meets the requirement of $K \geq 2$ changes slightly along with midtower longitudinal stiffness change. The two values are determined artificially according to the curve in the graph since only a range of μ is needed to divide different types of midtower. The intervals of longitudinal stiffness of different midtower types divided below are according to the value of μ required to meet the demand of sliding resistance coefficient.

Fig. 9(b) presents the effect of midtower longitudinal stiffness on the maximum vertical deflection-to-span ratio K_f and the horizontal line indicates the limit of $K_f \leq 1/250$ proposed in the code (CCCC Highway Consultants Co., Ltd.) (JTG/T-D65-05-2015 2015). As shown in Fig. 9(b), point A represents the value of midtower longitudinal stiffness corresponding to $K_f = 1/250$, therefore, the interval of midtower longitudinal stiffness that meets the limit of deflection-to-span ratio is $[Value\ A, +\infty]$. As shown in Fig. 9(a), point B represents the value of midtower longitudinal stiffness corresponding to $\mu = 0.19$ and $K = 2$, therefore, when $\mu = 0.19$, the interval of midtower longitudinal stiffness that meets the requirement of $K \geq 2$ is $(0, Value\ B]$, that is to say, the interval of midtower longitudinal stiffness, for which the maximum static friction coefficient required to meet the demand of $K \geq 2$ is 0.19, is $(0, Value\ B]$; similarly, the interval of midtower longitudinal stiffness, for which the maximum static friction coefficient required is 0.27 when $K \geq 2$ is $(Value\ B, Value\ C]$.

The intervals of longitudinal stiffness of different midtower types are derived from above analysis as shown in Table 3. The value range of rigid midtower for Oujiang River North Estuary Bridge is $(3.386 \times 10^5\ \text{kN/m}, +\infty]$. In the actual bridge, the midtower longitudinal stiffness of

Table 3 Intervals of longitudinal stiffness of different midtower types

Type	Interval of point position	Value range ($\times 10^5$ kN/m)
Rigid tower	$(Value\ C, +\infty]$	$(3.386, +\infty]$
Semi-rigid tower	$(Value\ B, Value\ C]$	$(0.823, 3.386]$
Flexible tower	$[Value\ A, Value\ B]$	$[0.180, 0.823]$

Oujiang River North Estuary Bridge is 4.382×10^5 kN/m, and according to Table 3, the midtower of Oujiang River North Estuary Bridge is rigid tower.

6. Rational longitudinal stiffness range for rigid midtower

The existing three-tower suspension bridges generally adopt a flexible midtower or a semi-rigid midtower. And investigations of stiffness for flexible and semi-rigid midtower have been made by several researchers (Yoshida *et al*. 2004, Wang and Chai 2018, Zhang and Fu 2014). However, there is no readily available information on the determination of rational longitudinal stiffness range for rigid midtower. In this section, rational range of rigid midtower longitudinal stiffness of Oujiang River North Estuary Bridge is further investigated with the value of the static friction coefficient μ varies from 0.28 to 0.3 after the interval of longitudinal stiffness of rigid midtower is obtained in previous section.

In the study of this section, the midtower longitudinal stiffness k ranges from 3.73×10^5 kN/m to 9.39×10^5 kN/m by changing D and B_1 as shown in Table 4, and all those values of stiffness belong to the interval of longitudinal stiffness of rigid midtower defined in Table 3. Fig. 10 illustrates the relationship of the maximum vertical deflection-to-span ratio K_f with sliding resistance coefficient K and midtower longitudinal stiffness when the static friction coefficient μ changes, and the horizontal line indicates the limit of sliding resistance coefficient. From Fig. 10 it can be seen that, (1) all the selected values of midtower longitudinal stiffness meets the requirement that $K_f \leq 1/250$; (2) when $\mu = 0.28$, point E is the value of midtower longitudinal stiffness corresponding to $K = 2$, that is to say, the rational range of longitudinal stiffness for rigid midtower is $(3.386 \times 10^5\ \text{kN/m}, Value\ E]$when $\mu = 0.28$; (3) when $\mu = 0.29$, point F is the value of midtower longitudinal stiffness corresponding to $K = 2$, therefore, the rational range of longitudinal stiffness for rigid midtower is $(3.386 \times 10^5\ \text{kN/m}, Value\ F]$ when $\mu = 0.29$; (4) when $\mu = 0.30$, all values in the range of rigid midtower stiffness meet the demand of $K \geq 2$, therefore, the rational range of longitudinal stiffness for rigid midtower is $(3.386 \times \frac{10^5 kN}{m}, +\infty]$ when $\mu = 0.30$; (5) the variation rate of sliding resistance coefficient changes very slightly with increase of midtower longitudinal stiffness in the selected value range, however, when there is a slight increase in static friction coefficient μ, the sliding resistance coefficient changes greatly, in other words, rational stiffness range of rigid midtower is remarkably enlarged.

Table 4 Structural parameters and corresponding midtower longitudinal stiffness*

D (m)	B_1 (m)	$k(\times 10^5$ kN/m)
25	8	3.73
30	6	4.00
30	7	4.38
30	8	4.99
35	6	5.32
35	7	5.92
35	8	6.52
35	9	7.12
35	10	7.73
40	8	7.99
40	9	8.69
40	10	9.39

**D*: the distance between centerlines of the two tower legs at the bottom in longitudinal direction; B_1: the width of each leg in longitudinal direction; *k:* the value of midtower longitudinal stiffness.

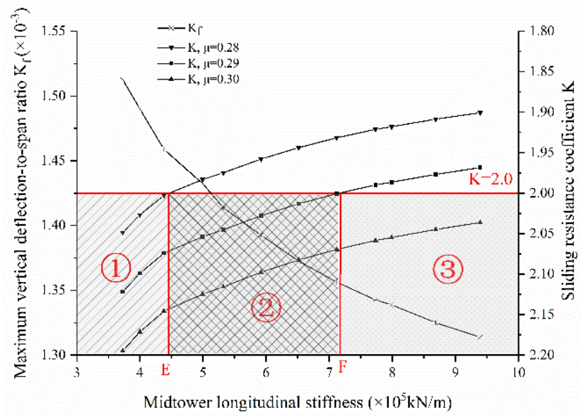

Fig. 10 Rational range of rigid midtower longitudinal stiffness with $\mu = 0.28 - 0.30$

The results above indicate that a rational range of rigid midtower longitudinal stiffness could be found under the limitation of the maximum vertical deflection-to-span ratio and sliding resistance coefficient. Since rigid midtower has a large value of longitudinal stiffness, it is easy to meet the requirement of the maximum vertical deflection-to-span ratio. Therefore, the key point of rigid midtower design is to meet the requirement of antiskid safety. Since static friction coefficient μ has an important impact on the sliding resistance coefficient, it is necessary to optimize the value of the maximum static friction coefficient. On the Oujiang River North Estuary Bridge, a test on the sliding performance of middle saddle was conducted, and the average friction coefficient from several test sets of multiple cables was greater than 0.3 by setting septum and partition wall in middle saddle. In addition, several research (Ji *et al*. 2009, Ruan *et al*. 2016, Zhang and Li 2013) indicates that it is possible to modify the value of static friction coefficient recommended in the code.

7. Conclusions

By taking the Oujiang River North Estuary Bridge as an example, this paper investigated the classification of different types of midtower and the determination of rational range for midtower stiffness. Based on the present study, the following conclusions are drawn:

• According to the relationship between midtower longitudinal stiffness and static friction coefficient, the midtower can be divided into three types, as: flexible tower, semi-rigid tower and rigid tower. The midtower longitudinal stiffness has a greater influence on K and K_f of a bridge with a flexible midtower than a bridge with a rigid midtower.

• The static friction coefficient μ has an important impact on rational longitudinal stiffness range. In other words, the rational longitudinal stiffness range of rigid midtower will be significantly enlarged with a small increase in μ. The selection of static friction coefficient requires an extensive study. However, based on this research, it is suggested that static friction coefficient μ could be 0.28-0.3 for the Oujiang River North Estuary Bridge considering the economy and applicability.

• It should be noted that the numerical method developed in this study does not consider dynamic and economic performance of the structure. Future studies should take these issues into consideration. Nevertheless, this research has produced some practical results for beginning to understand how to design midtower of three-tower suspension bridges.

Acknowledgments

This work presented herein has been supported by the National Key Research and Development Program of China under grant numbers 2018YFC0809600 and 2018YFC0809601, the Ministry of Science and Technology of China under grant number SLDRCE19-B-09 and the Fundamental Research Funds for the Central Universities under grant number 22120180316. The supports are gratefully acknowledged.

References

Cao, H.Y., Qian, X.D., Zhou, Y.L., Chen, Z.J. and Zhu, H.P. (2018), "Feasible range for midtower lateral stiffness in three-tower suspension bridges", *J. Bridge Eng.*, **23**(3), 06017009. https://doi.org/10.1061/(ASCE)BE.1943-5592.0001196.

Cheng, Z., Zhang, Q., Bao, Y., Jia, D., Bu, Y. and Li, Q. (2018), "Analytical study on frictional resistance between cable and saddle equipped with friction plates for multi-span suspension bridges", *J. Bridge Eng.*, **23**(1), 04017118. https://doi.org/10.1061/(ASCE)BE.1943-5592.0001176.

Choi, D.H., Gwon, S.G. and Na, H.S. (2014), "Simplified analysis for preliminary design of towers in suspension bridges", *J. Bridge Eng.*, **19**(3), 04013007. https://doi.org/10.1061/(ASCE)BE.1943-5592.0000551.

Choi, D.H., Gwon, S.G., Yoo, H. and Na, H.S. (2013), "Nonlinear static analysis of continuous multi-span suspension bridges", *Int. J. Steel Struct.*, **13**(1), 103-115. https://doi.org/10.1007/s13296-013-1010-0.

Collings, D. (2016), "Multiple-span suspension bridges: State of the art", *Proc., Inst. Civil Eng., Bridge Eng.*, **169**(3), 215-231. https://doi.org/10.1680/jbren.15.00035.

Daniel, R.A., van Dooren, F.J. and de Meijer, R.H. (2010), "Comparison of a single and double main span suspension bridge for the western Scheldt crossing", *IABSE Symp. Rep.*, **97**(35), 9-16.

Forsberg, T. (2001), "Multi-span suspension bridges", *Int. J. Steel Struct.*, **1**(1), 63-73.

Fukuda, T. (1967), "Analysis of multispan suspension bridges", *J. Struct. Div.*, **93**(3), 63-86.

Ge, Y.J. and Xiang, H.F. (2011), "Extension of bridging capacity of cable-supported bridges using double main spans or twin parallel decks solutions", *Struct. Eng. Mech.*, **7**, 551-567. https://doi.org/10.1080/15732479.2010.496980.

Hasegawa, K., Kojima, H., Sasaki, M. and Takena, K. (1995), "Frictional resistance between cable and saddle equipped with friction plate", *J. Struct. Eng.*, **121**(1), 1-14. https://doi.org/10.1061/(ASCE)0733-9445(1995)121:1(1).

Ji, L., Chen, C. and Feng, Z.X. (2007), "Study on slip resistance between main cable and saddle on middle tower of three-tower suspension bridge", *Highw.*, **6**, 1-6. https://doi.org/10.3969/j.issn.0451-0712.2007.06.001.

JTG-D60-2015 (2015), General Specifications for the Design of Highway Bridges and Culverts, CCCC Highway Consultants Co., Ltd., China Communications Press, Beijing, China.

JTG/T-D65-05-2015 (2015), Specifications for the Design of Highway Suspension Bridges, CCCC Highway Consultants Co., Ltd., China Communications Press, Beijing, China.

Jung, J., Kim, J., Baek, J. and Choi, H. (2010), "Practical design of continuous two main-span suspension bridge in Korea", *IABSE Symp. Rep.*, **97**(29), 62-69. https://doi.org/10.2749/222137810796024501.

Kim, H.S., Sohn, Y.K. and Yoo, D.H. (2012), "Parametric study on safety factor for cable slip in four-span suspension bridges", *IABSE Congress Rep., Int. Assoc. for Bridge and Structural Engineering*, Zurich. https://doi.org/10.2749/222137912805112158.

Ma, X., Nie, J. and Fan, J. (2016), "Longitudinal stiffness of multispan suspension bridges", *J. Bridge Eng.*, **21**(5), 06015010. https://doi.org/10.1061/(ASCE)BE.1943-5592.0000878.

Ruan, X., Zhou, J. and Caprani, C.C. (2016), "Safety assessment of the antisliding between the main cable and middle saddle of a three-pylon suspension bridge considering traffic load modeling", *J. Bridge Eng.*, **21**(10), 04016069. https://doi.org/10.1061/(ASCE)BE.1943-5592.0000927.

Takena, K., Sasaki, M., Hata, K. and Hasegawa, K. (1992), "Slip behavior of cable against saddle in suspension bridges", *J. Struct. Eng.*, **118**(2), 377-391. https://doi.org/10.1061/(ASCE)0733-9445(1992)118:2(377).

Thai, H.T. and Choi, D.H. (2013), "Advanced analysis of multi-span suspension bridges", *J. Constr. Steel Res.*, **90**, 29-41. https://doi.org/10.1016/j.jcsr.2013.07.015.

Wang, X.L. and Chai, S.B. (2018), "Determining the middle tower stiffness value in an in-plane double-cable triple-tower suspension bridge", *J. Bridge Eng.*, **23**(7), 06018001. https://doi.org/10.1061/(ASCE)BE.1943-5592.0001254.

Wang, X.L., Chai, S.B. and Xu, Y. (2017), "Sliding resistance of main cables in double-cable multispan suspension bridges", *J. Bridge Eng.*, **22**(3), 06016011. https://doi.org/10.1061/(ASCE)BE.1943-5592.0001018.

Yoshida, O., Okuda, M. and Moriya, T. (2004), "Structural characteristics and applicability of four-span suspension bridge", *J. Bridge Eng.*, **9**(5), 453-463. https://doi.org/10.1061/(ASCE)1084-0702(2004)9:5(453).

Zhang, L.W., Xiao, R.C., Jiang, Y. and Chai, S.B. (2012). "The characteristics of the multi-span suspension bridge with double main cables in the vertical plane", *Struct. Eng. Mech.*, **42**(3), 291-311. https://doi.org/10.12989/sem.2012.42.3.291.

Zhang, L.W., Xiao, R.C., Sun, B., Jiang, Y., Zhang, X.Y., Zhuang, D.L., Zhou, Y.G. and Tu, X. (2013), "Study on economic performances of multi-span suspension bridges part 1: simple estimation formulas", *Struct. Eng. Mech.*, **47**(2), 265-286. https://doi.org/10.12989/sem.2013.47.2.265.

Zhang, L.W., Xiao, R.C., Sun, B., Jiang, Y., Zhang, X.Y., Zhuang, D.L., Zhou, Y.G. and Tu, X. (2013), "Study on economic performances of multi-span suspension bridges part 2: parametric study", *Struct. Eng. Mech.*, **47**(2), 287-305. https://doi.org/10.12989/sem.2013.47.2.287.

Zhang, Q,H. and Li, Q. (2013), "Study on cable-saddle frictional characteristics of long-span suspension bridges", *China Civil Eng. J.*, **46**(4), 85-92. https://doi.org/10.15951/j.tmgcxb.2013.04.006.

Zhang, Q.H., Cheng, Z.Y., Cui, C., Bao, Y., He, J. and Li, Q. (2017), "Analytical model for frictional resistance between cable and saddle of suspension bridges equipped with vertical friction plates", *J. Bridge Eng.*, **22**(1), 04016103. https://doi.org/10.1061/(ASCE)BE.1943-5592.0000986.

Zhang, Q.H., Kang, J.P., Bao, Y., Cheng, Z.Y., Jia, D. L. and Bu, Y.Z. (2018), "Numerical study on cable-saddle frictional resistance of multispan suspension bridges", *J. Constr. Steel Res.*, **150**, 51-59. https://doi.org/10.1016/j.jcsr.2018.08.006.

Zhang, X.J. and Fu, G.N. (2014), "Seismic performance and its favorable structural system of three-tower suspension bridge", *Struct. Eng. Mech.*, **50**(2), 215-229. https://doi.org/10.12989/sem.2014.50.2.215.

CC